Thermal stability of photovoltaic a-Si:H determined by neutron reflectometry

A. J. Qviller, A. J. C. Dennison, H. Haug, C. C. You, I. M. Hasle, E. Østreng, H. Fjellvåg, A. Vorobiev, B. Hjörvarsson, E. S. Marstein, C. Frommen, and B. C. Hauback

---

Articles you may be interested in

Role of the buffer at the interface of intrinsic a-Si:H and p-type a-Si:H on amorphous/crystalline silicon heterojunction solar cells
Appl. Phys. Lett. **107**, 223901 (2015); 10.1063/1.4936196

Damage free laser ablation of SiO 2 for local contact opening on silicon solar cells using an a-Si:H buffer layer
J. Appl. Phys. **107**, 043518 (2010); 10.1063/1.3309382

Electrical transport mechanisms in a -Si : H / c -Si heterojunction solar cells
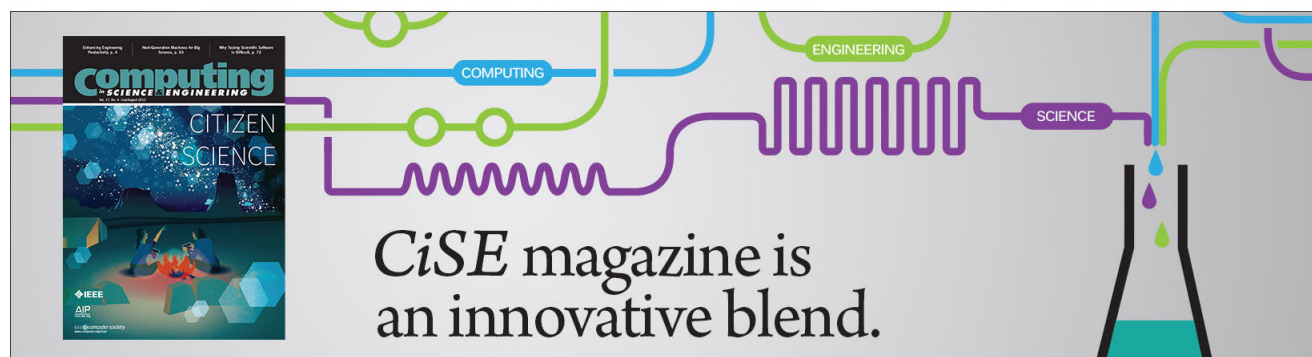J. Appl. Phys. **107**, 023711 (2010); 10.1063/1.3267316

Surface passivation of n-type crystalline Si by plasma-enhanced-chemical-vapor-deposited amorphous SiC x : H and amorphous SiC x N y : H films
Appl. Phys. Lett. **81**, 4461 (2002); 10.1063/1.1527230

Sensitization of the minority carrier lifetime in hydrogenated amorphous silicon
Appl. Phys. Lett. **72**, 103 (1998); 10.1063/1.120658

Thermal stability of photovoltaic a-Si:H determined by neutron reflectometry

A. J. Qviller,[1,a] A. J. C. Dennison,[2,3] H. Haug,[1] C. C. You,[1] I. M. Hasle,[1] E. Østreng,[4] H. Fjellvåg,[4] A. Vorobiev,[2,3] B. Hjörvarsson,[2] E. S. Marstein,[1] C. Frommen,[1] and B. C. Hauback[1]

[1]Institute for Energy Technology, P.O. Box 40, NO-2027 Kjeller, Norway
[2]Division for Materials Physics, Department of Physics and Astronomy, Uppsala University, Box 516, SE-751 20 Uppsala, Sweden
[3]Institut Laue-Langevin, 71 Avenue des Martyrs, 38000 Grenoble, France
[4]Department of Chemistry, Centre for Materials Science and Nanotechnology, University of Oslo, P.O. Box 1033, Blindern, NO-0315 Oslo, Norway

Neutron and X-ray reflectometry were used to determine the layer structure and hydrogen content of thin films of amorphous silicon (a-Si:H) deposited onto crystalline silicon (Si) wafers for surface passivation in solar cells. The combination of these two reflectometry techniques is well suited for non-destructive probing of the structure of a-Si:H due to being able to probe buried interfaces and having sub-nanometer resolution. Neutron reflectometry is also unique in its ability to allow determination of density gradients of light elements such as hydrogen (H). The neutron scattering contrast between Si and H is strong, making it possible to determine the H concentration in the deposited a-Si:H. In order to correlate the surface passivation properties supplied by the a-Si:H thin films, as quantified by obtainable effective minority carrier lifetime, photoconductance measurements were also performed. It is shown that the minority carrier lifetime falls sharply when H has been desorbed from a-Si:H by annealing. © 2014 AIP Publishing LLC.
[http://dx.doi.org/10.1063/1.4904340]

To reduce the costs of solar electricity, much effort is devoted to the development of more efficient crystalline silicon (Si) solar cells, which is the most important solar cell technology today. Key components of all high efficiency solar cell architectures based on Si are the surface passivation layers: dielectric material systems that reduce minority carrier recombination at the silicon wafer surfaces. A commonly used material is amorphous and hydrogenated Si (a-Si:H) made by plasma-enhanced chemical vapour deposition (PECVD).[1] In this material, hydrogen (H) plays an important role in defining the surface passivation properties. Although widely used in the manufacture of heterojunction solar cells, the use of a-Si:H in other solar cell architectures is limited by the low thermal stability of the material.[2] To allow for the development of improved deposition processes for a-Si:H resulting in films with both improved surface passivation properties and improved thermal stability, we have investigated surface passivated a-Si:H films before and after thermal treatment by photoconductance minority carrier lifetime measurements, as well as by neutron reflectivity (NR) and X-ray reflectivity (XRR) measurements.

Passivated a-Si:H films investigated in this study were deposited onto n-type silicon float-zone wafers with ⟨100⟩ orientation. Prior to deposition, the wafers were dipped in hydrogen fluoride (HF) (5%) and rinsed in de-ionized water. Thereafter, approximately 40 nm of a-Si:H was deposited onto both sides of the wafer in an Oxford Systems PlasmaLab 133 PECVD reactor at 230 °C using silane (SiH_4). A rapid thermal processing (RTP) system (AccuThermo AW610) was used to anneal the wafers at specific temperatures for 1 min at steady state. Minority carrier lifetime was measured using a WTC-120 Photoconductance Lifetime Tester from Sinton Instruments. A series of such measurements for a-Si:H samples annealed at different temperatures in order to desorb hydrogen is shown in Fig. 1. Two samples of a-Si:H on $2 \times 2\,cm^2$ Si substrates were selected for XRR and NR measurements. One of the samples was annealed at 500 °C for 1 min the same day as the NR measurement took place. The other sample was only exposed to room temperature after deposition and used as a pristine reference sample.
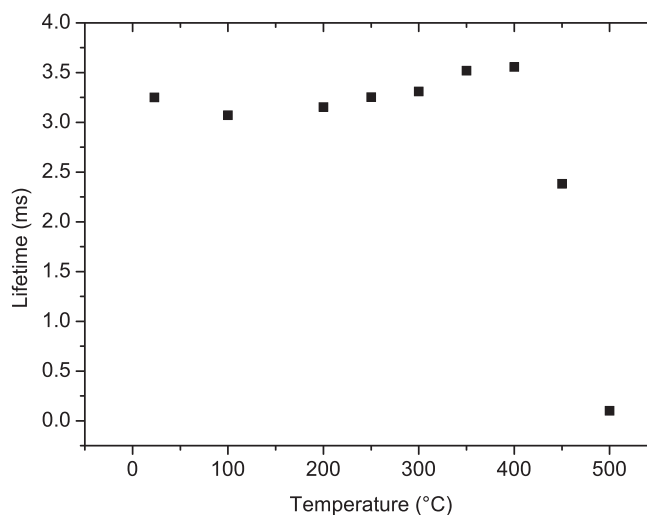

FIG. 1. Minority carrier lifetime measurements on a series of 40 nm a-Si:H/Si bilayers annealed at different temperatures. The uncertainty is a few percent.

a)Author to whom correspondence should be addressed. Electronic mail: atlejq@ife.no

The goal of a reflectometry experiment is to determine the scattering length density (SLD) as a function of depth z from the surface. For neutrons, the SLD is defined as

$$SLD = \frac{1}{\phi} \sum_i n_i b_i, \tag{1}$$

where n_i is the number of atoms in a molecule and b_i is the coherent scattering length for element i. The quantity ϕ is the molecular volume. For X-rays, the SLD is simply the volume average of the elements' electron density. Reflectometry suffers from the phase problem that is generic to all scattering techniques, meaning that different SLD profiles may give rise to identical or almost identical reflectivity profiles.[3] Knowledge of the layer ordering and performing both NR and XRR measurements is one way to exclude incorrect interpretation of results. XRR is sensitive to the electron density of the material in question and thus light elements, especially H, are invisible to this technique. In the present a-Si:H thin films, XRR has two weaknesses: First, the insensitivity to the H content; and second, the poor contrast between Si and SiO_2 resulting from surface oxidation. Thus, the combination of NR and XRR is highly beneficial as XRR gives accurate determination of the layer thicknesses, while the NR provides information about the thickness and the composition.

A PANalytical X-ray reflectometer operating at the Cu K_a wavelength $\lambda = 1.542\,\text{Å}$ was used for the XRR measurements. The reflectivity R was measured at the specular condition as a function of 2θ in the angular range $2\theta = 0°-12°$ for 1 h. NR was performed at the SuperADAM neutron reflectometer situated at Institute Laue-Langevin, Grenoble, France,[4] at a wavelength $\lambda = 4.4\,\text{Å}$ and with wavelength dispersion $(\Delta\lambda/\lambda) = 0.007$. The reflectivity $R(\theta)$ was measured for each sample at the specular condition $2\theta = 0°-8°$ for 8 h. Reflectivity data together with sample model fits are plotted as a function of the transferred momentum $q = 4\pi\lambda^{-1}\sin\theta$ in Figs. 2(a) and 2(b), for the XRR and NR data, respectively.

The data were analyzed using the GenX reflectivity fitting package.[5] NR and XRR data were simultaneously refined using the logarithm of the reflectivity as the figure of merit. In addition, the square root of the reflectivity and the chi square of the data were also tried. However, these figures of merit overemphasize the region near the critical angle where systematic errors are known to be worst and therefore gave inferior results. A four layer model for the surface structure was constructed as it has proven impossible to simultaneously fit both datasets well with just three layers due to different q-ranges and element sensitivities of the NR and XRR measurements. In particular, the low frequency oscillation in the XRR data is outside the q-range of the NR data, while the internal H distribution is invisible to the XRR. In this four layer model, the contribution to the electron density caused by H was assumed to be negligible. The model was constructed for the X-rays so that the bottom two layers were composed of pure Si and the top two of SiO_2. The density, thickness, and roughness of these layers were varied during the fitting process. For the NR data, an additional parameter was the coherent scattering length per formula unit.
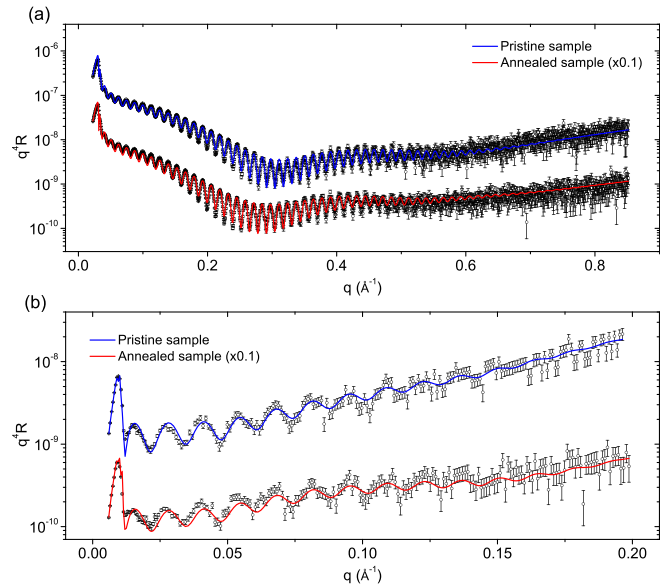

FIG. 2. (a) XRR profiles and model fits for the pristine sample and the sample annealed at 500 °C. (b) NR profiles and model fits. The graphs are offset by a factor of 0.1 for clarity. In parts of the figures, the statistical error bars are smaller than the model fit lines.

As previously mentioned, XRR has very poor contrast between SiO_2 and Si, but NR can distinguish well between all different materials present in the sample. X-rays are, in particular, powerful to determine total thickness and surface roughness, and XRR could resolve a thin layer of around 1 nm at the solid-air interface which appeared to have an extremely low density for SiO_2. The density of this layer can be explained as being a non-Gaussian roughness at this interface and the value being composed of the SLD for both air and SiO_2. Below this layer, the model includes a slightly thicker layer of SiO_2 with the same density and thus similar X-ray SLD as the a-Si:H layers.

A broad interface is observed in the pristine and annealed samples underneath the oxide layers. Ascertaining the composition of this layer is, however, complicated by the possible presence of the three elements Si, O, and H. Since the value of the neutron SLD of this layer lies between that for pure Si and SiO_2, we would hypothesize that this interface does contain some oxygen. X-ray and neutron SLD profiles are shown in Fig. 3.

Hydrogen has a negative scattering length b and thermal processes resulting in desorption of H will therefore cause an increase of the a-Si:H SLD. When regarding the neutron SLDs in Fig. 3, it is clearly seen that the neutron SLD of the innermost a-Si:H layer in the annealed sample is higher than the innermost layer in the pristine sample. Good fits to the neutron reflectivity data are obtained with a $SLD = 1.597 \times 10^{-6}\,\text{Å}^{-2}$ of this innermost a-Si:H layer in the pristine sample and a $SLD = 1.744 \times 10^{-6}\,\text{Å}^{-2}$ of the corresponding a-Si:H layer in the annealed sample. The respective densities of these layers, as obtained from XRR are $\rho = 2.160\,\text{g/cm}^3$ and $\rho = 2.119\,\text{g/cm}^3$, while the crystalline Si substrate has a density of $\rho = 2.330\,\text{g/cm}^3$.

The definition of the SLD, Eq. (1), may be rearranged in order to solve for the number of H atoms per Si atom in the innermost a-Si:H layer. In order to do this, one uses $\phi =$
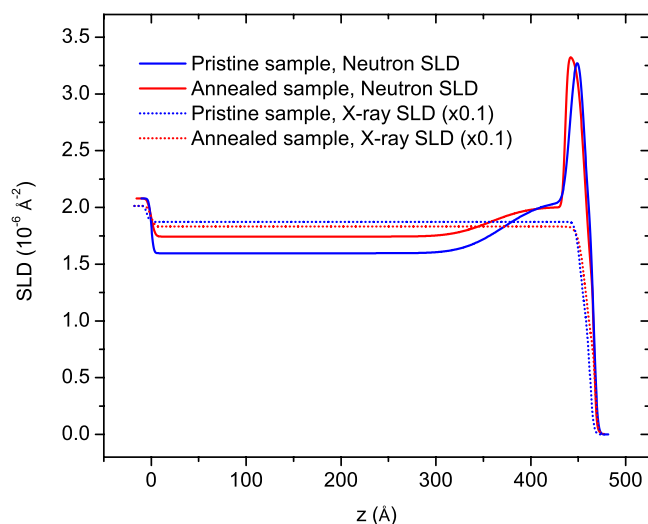
FIG. 3. X-ray and neutron SLD profiles of the 40 nm pristine sample and the 40 nm sample annealed at 500 °C. The X-ray SLDs are multiplied with a factor of 0.1 to fit into the same figure as the neutron SLDs.

$M_R/\rho N_A$ for the molecular volume with Si formula mass $M_R = 28.09$, Si density ρ, and Avogadro's number N_A. It is also assumed that H does not contribute to the density ρ and formula mass M_R. By setting $n_{Si} = 1$, Eq. (1) is then rearranged into

$$n_H = \frac{SLD \times \phi - b_{Si}}{b_H}, \qquad (2)$$

where n_H is now the number of H atoms per Si atom. In addition to the a-Si:H layer SLD, the molecular volume ϕ calculated with ρ obtained from the XRR data and tabulated coherent scattering lengths $b_{Si} = 4.1491$ fm and

$b_H = -3.7390$ fm are used in Eq. (2) to determine this ratio for both samples. For the pristine sample, the calculation yields $n_H = 0.18$, while the result for the annealed sample is $n_H = 0.08$. Thus, approximately half of the H content been desorbed from the a-Si:H thin films as a result of the thermal processing. It is clearly seen from Fig. 1 that this is strongly correlated with significant reduction of minority carrier lifetime of the sample depleted of H after annealing at 500 °C.

In this work, a clear connection between long minority carrier lifetimes and the presence of H in thin films of a-Si:H/Si deposited on Si has been shown by NR, XRR, and photoconductance measurements. The results are consistent with the assumption that H plays a significant role in passivation. Further work will focus on the intermediate temperature regime and different a-Si:H layer thicknesses.

[1] S. De Wolf, A. Descoeudres, Z. C. Holman, and C. Ballif, "High-efficiency silicon heterojunction solar cells: A review," Green **2**(1), 7–24 (2012).
[2] H. Li and S. R. Wenham, "Influence of a-Si:H deposition power on surface passivation property and thermal stability of a-Si:H/SiNx:H stacks," AIP Adv. **2**(2), 022106 (2012).
[3] J. Daillant and A. Gibaud, *X-ray and Neutron Reflectivity* (Springer, 2010), p. 117.
[4] A. Devishvili, K. Zhernenkov, A. J. C. Dennison, B. P. Toperverg, M. Wolff, B. Hjörvarsson, and H. Zabel, Rev. Sci. Instrum. **84**(2), 025112 (2013).
[5] M. Björck and G. Andersson, J. Appl. Cryst. **40**, 1174 (2007).